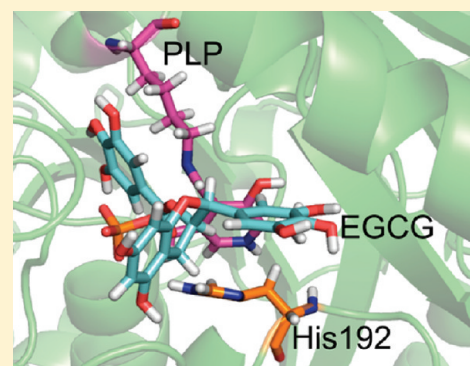


# Structural Perspective on the Direct Inhibition Mechanism of EGCG on Mammalian Histidine Decarboxylase and DOPA Decarboxylase

M. Victoria Ruiz-Pérez,<sup>†</sup> Almudena Pino-Ángeles,<sup>†</sup> Miguel A. Medina, Francisca Sánchez-Jiménez, and Aurelio A. Moya-García\*

Departamento de Biología Molecular y Bioquímica, Facultad de Ciencias, Universidad de Málaga, Málaga, Spain and CIBER de Enfermedades Raras (CIBERER), Valencia, Spain

**ABSTRACT:** Histidine decarboxylase (HDC) and L-aromatic amino acid decarboxylase (DDC) are homologous enzymes that are responsible for the synthesis of important neuroactive amines related to inflammatory, neurodegenerative, and neoplastic diseases. Epigallocatechin-3-gallate (EGCG), the most abundant catechin in green tea, has been shown to target histamine-producing cells and to promote anti-inflammatory, antitumor, and antiangiogenic effects. Previous experimental work has demonstrated that EGCG has a direct inhibitory effect on both HDC and DDC. In this study, we investigated the binding modes of EGCG to HDC and DDC as a first step for designing new polyphenol-based HDC/DDC-specific inhibitors.



## INTRODUCTION

Tea is the second most-consumed beverage in the world, made from the leaves and buds of *Camellia sinensis*. There are many different types of tea, and their classification is based on the manufacturing processes used to produce them. Among these, green tea has been commonly associated to a healthy condition. The Chinese have traditionally used it for treating headache, physical pain, and depression, to improve digestion, and for detoxification of the organism. In addition, green tea is an energizing product and, in general, has been thought to prolong life. These medicinal properties have been validated by scientific evidence in recent years.<sup>1–4</sup>

Tea is a natural source for several different secondary metabolism products, including the amino acid theanine, methylxanthines, such as caffeine and theobromine, polyphenolic antioxidants, and flavonoids, such as catechins (flavan-3-ols). There are four major catechins present in green tea: (–)-epigallocatechin-3-gallate (EGCG; Figure 1), (–)-epigallocatechin, (–)-epicatechin-3-gallate, and (–)-epicatechin, being EGCG the most abundant one in green tea (59%).<sup>5</sup> EGCG has been shown to target histamine-producing cells affecting to their proliferation, adhesion, migration, and invasion potential.<sup>6,7</sup> Hence, EGCG is considered a potent anti-inflammatory, antitumor, and antiangiogenic effector.<sup>5,8–12</sup>

It has been demonstrated that EGCG is able to bind and inhibit multiple molecular targets, including histidine decarboxylase (HDC, EC 4.1.1.22),<sup>13</sup> the enzyme responsible for production of histamine, and L-aromatic amino acid decarboxylase or 3,4-dihydroxyphenylalanine (DOPA) decarboxylase (DDC, EC 4.1.1.28), the enzyme

responsible for synthesis of several neurotransmitters, such as serotonin and dopamine.<sup>14</sup>

HDC and DDC are homodimeric, homologous enzymes that share over 50% sequence identity. They belong to the group II of L-amino acid decarboxylases. The quaternary structures of these decarboxylases share many conserved features, including a similar active site conformation, as previously reviewed by our group.<sup>15–17</sup>

In the absence of substrate or inhibitors, the UV–vis absorption spectra for both mammalian HDC and DDC are similar; the cofactor, pyridoxal 5′-phosphate (PLP), is bound to a conserved lysine residue via a Schiff base with two tautomeric forms, so the absorption spectra for both enzymes contains two maxima, which correspond to the major enolimine tautomer (335 nm) and the ketoenamine (425 nm) form.<sup>18,19</sup> Association of EGCG with DDC and HDC causes a similar change in the absorption spectra in both enzymes, indicating that this polyphenol could elicit similar conformational changes in the environment of PLP. In particular, EGCG causes the disappearance of the absorbance peak at 425 nm, which corresponds to the ketoenamine form of the Schiff base between PLP and the protein. DDC activity can be recovered by addition of L-DOPA, which is a natural substrate of the enzyme, but not through a gel filtration process. Furthermore, D-DOPA, an active site-directed inhibitor of DDC, prevents inactivation of the enzyme mediated via EGCG.<sup>14</sup> Although it seems clear that EGCG binds to the active site of HDC, we cannot be sure whether conformational changes can be

Received: May 19, 2011

Published: November 22, 2011

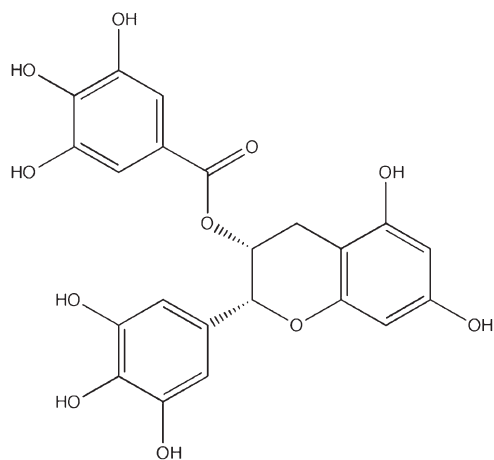


**Figure 1.** (—) Epigallocatechin-3-gallate (EGCG) structure. EGCG is an antioxidant polyphenol and the major catechin present in green tea.

transmitted along the structure of the enzyme or not.<sup>20</sup> Therefore, locating the binding site for EGCG in these decarboxylases and unveiling how this event affects their dynamic behavior could be helpful in the search for new modulators of these activities and for developing new strategies to control rare or emergent pathologies such as allergies,<sup>21,22</sup> Parkinson's disease,<sup>23–25</sup> and Alzheimer's disease,<sup>26–28</sup> in which both enzymes are directly implicated.

In the present work, we describe a computational study to determine how EGCG binds to HDC and DDC. The most promising results from the docking experiments were selected in order to build the enzyme–ligand complexes, and their stability and conformational changes were studied by means of molecular dynamics (MD) simulations. Analyses of the simulations revealed that one of the EGCG poses, which is located close to the active site of both enzymes, exerts an important conformational change in their active sites and that this conformational change could prevent the substrate from binding into the active site.

## MATERIALS AND METHODS

**Systems Construction.** We used the structures of both PLP-dependent decarboxylases, HDC and DDC, as receptors in the docking experiments. Both enzymes were used in their internal aldimine conformation in which the cofactor is bound to a lysine residue within the active site, resembling an unbound state. The dimeric structure of DDC was retrieved from the Protein Data Bank (accession 1JS6),<sup>23</sup> and we used a homology model for the HDC structure.<sup>16,17</sup> The Autodock Tools (ADT) software package<sup>29</sup> was used to prepare both the ligand (EGCG) and the receptors for docking. For the ligand, Gasteiger charges were calculated and the active torsions selected. For the receptors, the nonpolar hydrogens were eliminated and the Gasteiger charges loaded. The protonation states of the residues within the two enzymes were calculated via the H++ server<sup>30</sup> using the Generalized Born method; we applied the default parameters, except for the internal dielectric constant, which was set to 4. These protonation states in the dimerization surface were also visually checked for both proteins, special attention being given to histidine residues.

**Ligand–Protein Docking.** Docking experiments were conducted with AutoDock 4<sup>29</sup> on a Linux workstation (SuSE 10.0)

with an AMD 64 bit 3.7 GHz CPU and 2 GB of RAM. File preparation and data analyses were conducted using an iMac PowerPC G5 with a 1.8 GHz CPU, 2 GB of RAM, and running the MacOS X 10.5.5 operating system.

ADT was also used for defining the location and size of the docking grids. For each enzyme, two grids were generated. The first grid was placed over the entire dimerization surface of one monomer, whereas the second grid was located over the entrance channel to the active site of each dimeric enzyme. All of the docking grids were built using a default spacing value of 0.375 Å. The grids were used in AutoGrid 4 (part of the AutoDock 4 software) to calculate affinity and electrostatic maps. Finally, the docking simulations were conducted via a Lamarckian Genetic Algorithm using default parameters, except in the following cases: *ga\_num\_evals* (maximum number of energy evaluations), 25000000; *ga\_num\_generations* (maximum number of generations), 27000; and *ga\_run* (number of hybrid Genetic Algorithm–Local Search runs), 50. Only ligand flexibility was taken into account, and the proteins were considered to be rigid bodies. The resulting complexes were clustered according to their root mean square deviation (rmsd) values and binding energies, which were calculated using the Autodock scoring function. We found two different ways of EGCG binding to monomeric HDC. In one of them EGCG was docked next to the HDC active site, while in the other EGCG was docked to the dimerization surface of HDC. We built HDC dimers from these EGCG–HDC monomeric complexes using the GRAMM docking software.<sup>31</sup> We calculated rmsd from the original dimer structure using ProFit for the 1000 dimer structures generated with GRAMM. The best dimer structures were selected according to rmsd and GRAMM Energy values. The EGCG-docked conformations for the complex with DDC were selected using the same criteria. Further characterization via molecular dynamics (MD) simulations was conducted using complexes that were selected according to their binding energy values and the interactions made with the surrounding residues.

**Complex Refinement Using Molecular Dynamics Simulations.** The dimeric decarboxylase–EGCG complexes (HDC/DDC–EGCG) were refined via MD simulations following a protocol that we described previously.<sup>17</sup> Briefly, the simulations were run using the program AMBER<sup>32</sup> under the Amber force field ff03. All of the systems were solvated in a 12 Å edge truncated octahedron of TIP3P water molecules<sup>33</sup> and neutralized with counterions. The particle mesh Ewald (PME)<sup>34</sup> was used to treat the long-range interactions. The energy minimization protocol consisted of three independent stages, all of which used 50 steps of steepest descent followed by 950 steps with the conjugate gradient algorithm as follows: minimization of the hydrogen atoms only, minimization of the water molecules and ions only, and minimization of the entire system. The systems were heated to 300 K and equilibrated for 100 ps. Each of the MD simulations were subsequently extended for 15 ns, whereupon coordinates were saved every 1 ps, thereby providing a total of 15 000 snapshots. The trajectories were processed using the ptraj module in the AMBER package and visually inspected via VMD.<sup>35</sup>

**Ligand Binding Analysis.** rmsd and energy values along the trajectories were used as references to determine at which point along the trajectories the structures were stabilized. An average structure for the last nanosecond in the trajectory of each of the four HDC/DDC–EGCG complexes was generated using ptraj, and the geometry of each was optimized by energy minimization (1000 steps using the steepest descent algorithm). The HDC–EGCG

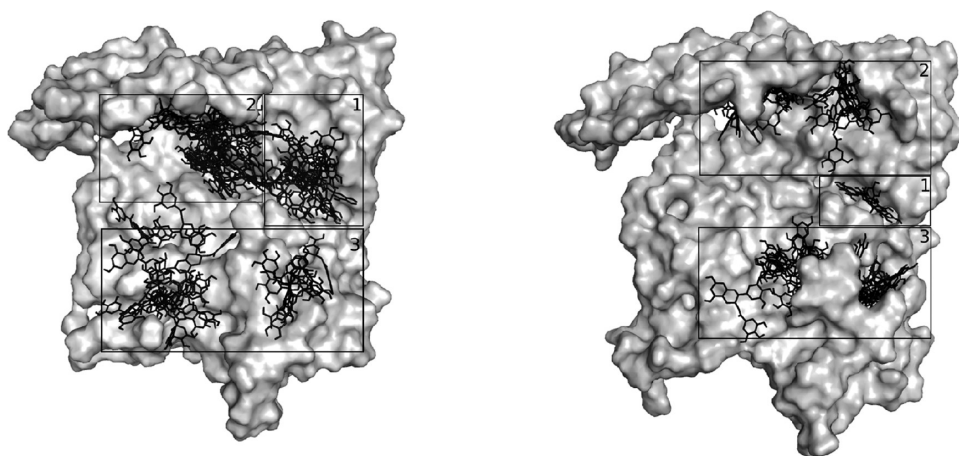


**Figure 2.** EGCG-docked conformations: DDC (left) and HDC (right). Monomers are depicted as gray surfaces and EGCG-docked conformations as black sticks. Regions 1–3 are equivalent between both enzymes. One docked conformation was selected in each region for further analysis. Only the best docked structure on region 1 was promising enough for deeper characterization.

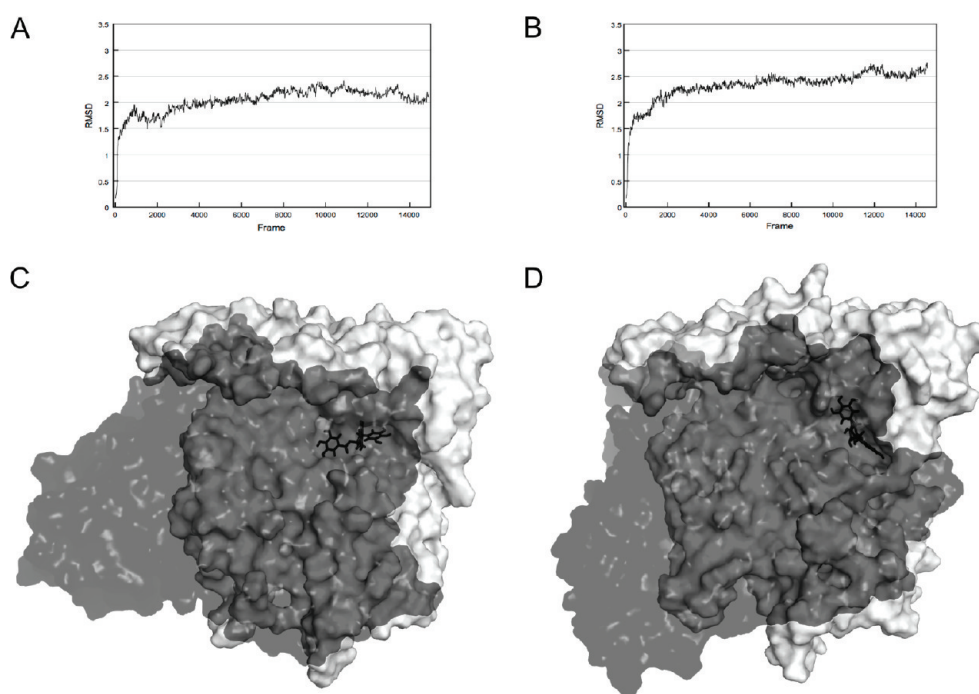


**Figure 3.** (A and B) DDC and HDC rmsd values along the MD trajectories. In both cases structures reach stabilization around 2–2.5 Å after 2 ns of simulation. (C and D) EGCG docked in DDC and HDC. These complexes were used in the MD simulations mentioned above. EGCG takes up the space in both enzymes substrate-binding pockets, plugging the active site entrances. Enzymes monomers are depicted as surfaces in white and transparent black; EGCG is shown as black sticks.

complex was used in a docking experiment in which the HDC substrate (histidine) and two known inhibitors (histidine methyl ester and  $\alpha$ -fluoromethyl histidine) were tested to assess whether they could bind to the enzyme active site in the presence of EGCG. This docking process was conducted on the automated platform VSDMIP<sup>36</sup> following a previously published protocol.<sup>37</sup>

## RESULTS

**EGCG Docking to HDC and DDC.** For both enzymes, the active sites are located in the dimerization surface, as described previously.<sup>15</sup> In previous experiments, it has been already

demonstrated that EGCG binding distorted the internal aldimine (E-PLP) spectrum, which was notably sensitive to polarity changes in its environment.<sup>19</sup> Thus, EGCG binding to the dimerization surface could have an impact on both the active site conformation and the E-PLP spectral properties. As a first approach to determine the feasible interaction modes for EGCG with the DDC and HDC structures, we conducted a blind docking experiment over the entire dimerization surface for one of the two monomers of each enzyme. The 50 docked conformations obtained for each enzyme were grouped into 3 regions along the HDC and DDC surfaces (Figure 2).



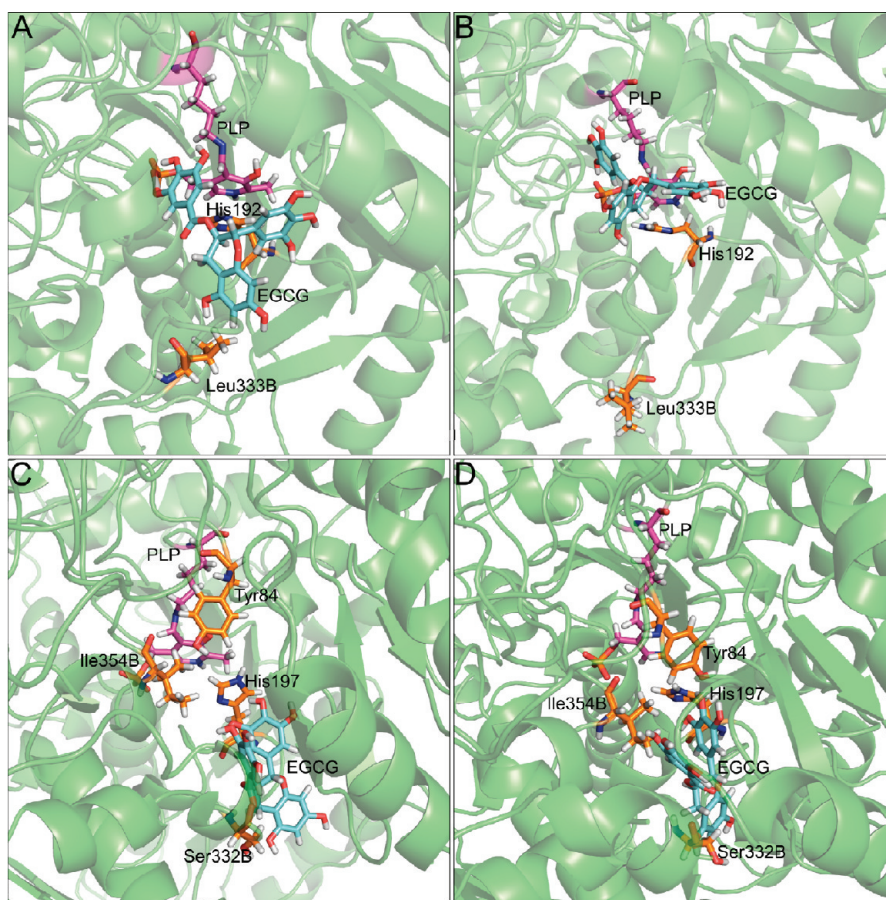


**Figure 4.** Details of the beginning and end of the MD simulations in DDC and HDC active sites, respectively. Residues named as “B” after their number in the sequence indicates they belong to a different monomer of the dimeric enzyme. (A and B) EGCG moves deeper in DDC active site, losing contact with the residue Leu333B. (C and D) Presence of EGCG causes residues Ile354B and Tyr84 to move toward the active site in HDC, collapsing the substrate-binding pocket.

The best-docked conformations for each region were selected according to its binding energy and the interactions that were made with the surrounding residues in the protein. The docking of EGCG in regions 2 and 3 of both HDC and DDC showed a low deviation from the original complex in the structural analysis with ProFit. These results indicate that EGCG causes no relevant perturbation in either the overall quaternary structures or the active site conformations of any of the dimeric enzymes. On the other hand, since experimental data shows that EGCG affects the active site environment in both enzymes, we focused on the study of the complexes in which EGCG interacts with the residues comprising both HDC and DDC active sites, which were the best-docked conformations in region 1 (Figure 2).

In region 1, EGCG partially occluded the substrate entrance within HDC and established hydrogen bonds with the highly conserved residue His197 and several residues in a functional loop of the opposite monomer,<sup>17</sup> i.e., Ser332. As the active site in DDC was more exposed to the solvent than the active site in HDC,<sup>15,19</sup> it was not surprising that EGCG could make interactions deeper into the binding pocket with the essential residue His192 (the counterpart of HDC His197) and Leu333 in the homologous functional loop and even with the cofactor.

**HDC–EGCG and DDC–EGCG Complex Refinements.** We performed 15 ns long MD simulations to ensure proper conformational space sampling for each complex, as shown in Figure 3. rmsd

values for the structures along the trajectories ( $C\alpha$  atoms) were calculated using the coordinates after the heating process as a reference. Analysis of the HDC–EGCG complex showed that the structure reached an rmsd value of 2 Å after 2 ns of simulation and subsequently stabilized at approximately 2.5 Å rmsd just after the first 6 ns of simulation (Figure 3B). These first results confirmed that EGCG does not alter the HDC dimeric structure. Furthermore, visual inspection of the MD trajectories revealed no major conformational changes in the overall quaternary structure of any of the complexes. We observed that the presence of EGCG contiguous to the active site entrance led to the movement of several residues in the HDC active site (Figure 4). EGCG occluded the entrance channel to the enzyme active site and established new interactions with residues in the active site. These residues turned outward when the active site collapsed. These rearrangements and the consequent collapse of the binding pocket occurred rapidly within the simulation time frame.

Regarding the DDC–EGCG simulation, the rmsd values along the trajectory showed an overall stabilization of the structure at approximately 2–2.4 Å (Figure 3A). We observed a similar behavior to that of the HDC–EGCG complex: EGCG did not affect the quaternary structure of the enzyme and remained stable in the active site throughout the entire trajectory. After 700 ps of simulation, EGCG moved deeper into the active site: its two catechol rings that were previously exposed to the

binding site entrance are then relocated inside the active site. While adopting this conformation, EGCG actually filled the binding pocket and blocked its entrance pathway.

**Docking of Known HDC Ligands in the Presence of EGCG.** To test the relevance of the movements described above for the substrate binding process, we established a single docking experiment with flexible ligands using the VSDMIP platform. Our ligands were histidine (the natural substrate for HDC) and the inhibitors histidine methyl ester and  $\alpha$ -fluoromethyl histidine. They were subsequently docked into the active site of the HDC–EGCG complex, and none of them were able to bind into the HDC binding site. We also observed that EGCG established new interactions with the residues in the active site Tyr84, Arg450, and Ile354B, thus reducing the volume of the substrate-binding pocket. Therefore, the binding of EGCG to the vicinity of the active site resulted in a conformational change at the residue level that led to shrinkage of the substrate-binding pocket.

## DISCUSSION AND CONCLUSIONS

There are more than 200 different human cell types, and among them, only a small subset is able to produce histamine. These cells include neurons, enterochromaffin-like cells, gastrin-containing cells, and many immune cells;<sup>38</sup> hence, histamine is involved in many different physiological processes, and deregulation of its metabolism is closely related to many prevalent, emergent, and rare diseases. These diseases are primarily described as inflammation-dependent pathologies and include mastocytosis, basophilic leukemia, gastric ulcer, Crohn's disease, and other inflammatory bowel diseases. Furthermore, oncogenic transformation has been shown to switch certain nonhistamine-producing cells to a histamine-producing phenotype, as occurs in the cases of melanoma, small cell lung carcinoma, and several types of neuroendocrine tumors.<sup>39,40</sup> Modulation of histamine action is an important pharmacological topic, and most of the current research on this area has been focused on blocking histamine binding to one of its four known membrane receptors. Although it is possible that selective, direct inhibition of HDC could have secondary effects, control of histamine production may be relevant in the treatment of conditions in which either local or circulating levels of histamine are excessive due to abnormal histamine production.

Dopamine and serotonin are two important neurotransmitters in the mammalian nervous system. Dopamine deficits in the substantia nigra of the brain are thought to be the cause of Parkinson's disease,<sup>41</sup> whereas a serotonin deficit has been associated to sleep, mood, depression, and anxiety disorders.<sup>42–45</sup> Because DDC is involved in the biosynthesis of these neurotransmitters, this enzyme has been implicated in a number of clinical disorders, including Parkinson's disease and hypertension. A common strategy for treatment of Parkinson's disease has been the administration of L-DOPA; however, as L-DOPA is rapidly converted to dopamine in the bloodstream, it is routinely administered with a DDC inhibitor that cannot cross the brain–blood barrier; thus, greater amounts of L-DOPA can reach the brain.

In this paper, we report a detailed model for the interaction between EGCG and the enzymes HDC and DDC. We found that EGCG flips within the substrate-binding pocket of DDC and forms hydrogen bonds with the cofactor PLP and Thr246 (Figure 4). In a previous work Bertoldi and co-workers concluded that DDC inhibition mediated by EGCG occurs as a

result of an interaction in the active site, probably near the PLP binding site and without PLP release, as shown in the absorption spectrum changes for the enzyme after addition of EGCG.<sup>14</sup> Although it was suggested that inhibition could take place via a covalent interaction, it was not unequivocally proven. Our results are in agreement with the former conclusion, as the docking experiments and MD simulations have shown that EGCG binds inside the DDC active site, where it forms important hydrogen bonds with several residues in the binding pocket; for example, residue Thr246 has been proven to be essential in catalyzing the oxidative deamination of aromatic amines in DDC.<sup>46</sup>

Regarding HDC, EGCG is able to establish hydrogen bonds with residues Tyr84, Pro440, and Ser332. As shown in Figure 4, EGCG causes Tyr84 to move toward the binding pocket and contact His197, which is a highly conserved residue, nonessential for enzymatic activity,<sup>47</sup> but it is an important factor in the correct positioning of PLP within HDC.<sup>16</sup> Ser332 is part of the flexible loop (residues 331–348), a key structural element in HDC catalysis and stability.<sup>37</sup> Thus, EGCG seems to alter the conformational properties important for PLP positioning, substrate binding, and catalysis according to our results.

In summary, our results suggest that EGCG does not distort the quaternary structures of HDC and DDC, and the dimerization surface appears to be a poor target for the modulation of histamine and dopamine production by polyphenols. The mechanism for the inhibitory effect of EGCG is based on alterations of the chemical environment in the active site of both enzymes and physical occlusion of the substrate entrance. This mechanism suggests that the active sites of DDC and HDC are the primary areas for EGCG inhibitory activity and indicates that these sites would be good targets for design of inhibitors with the pharmacological potential to treat Parkinson's disease, inflammatory conditions, and cancer.

## AUTHOR INFORMATION

### Corresponding Author

\*E-mail: amoyag@uma.es.

### Author Contributions

<sup>†</sup>These authors contributed equally.

## ACKNOWLEDGMENT

We thank Dr. Rubén Gil Redondo for his help with the virtual screening process. This work was supported mainly by CIBER de Enfermedades Raras, CIBERER (A.P.A. is a predoctoral researcher at CIBERER, and M.V.R.P. was a recipient of a CIBERER shuttle fellowship), as well as grants SAF2008-02522, SAF2011-26528 351, and PS09/02216 (MICINN, ISCIII and FEDER) and funds from Junta de Andalucía, BIO-267 and P07-CVI-02999 (co-funded by FEDER). The CIBER de Enfermedades Raras is an initiative of the ISCIII. The authors thank the Plataforma Andaluza de Bioinformática for computational support.

## REFERENCES

- (1) Khan, N.; Adhami, V. M.; Mukhtar, H. Review: green tea polyphenols in chemoprevention of prostate cancer: preclinical and clinical studies. *Nutr. Cancer* **2009**, *61*, 836–841.
- (2) Moore, R. J.; Jackson, K. G.; Minihane, A. M. Green tea (*Camellia sinensis*) catechins and vascular function. *Br. J. Nutr.* **2009**, *102*, 1790–1802.



- (3) Grove, K. A.; Lambert, J. D. Laboratory, epidemiological, and human intervention studies show that tea (*Camellia sinensis*) may be useful in the prevention of obesity. *J. Nutr.* **2010**, *140*, 446–453.
- (4) Melgarejo, E.; Urdiales, J. L.; Sánchez-Jiménez, F.; Medina, M. A. Targeting polyamines and biogenic amines by green tea epigallocatechin-3-gallate. *Amino Acids* **2010**, *38*, 519–523.
- (5) Cabrera, C.; Artacho, R.; Giménez, R. Beneficial effects of green tea—a review. *J. Am. Coll. Nutr.* **2006**, *25*, 79–99.
- (6) Melgarejo, E.; Medina, M. A.; Sánchez-Jiménez, F.; Botana, L. M.; Dominguez, M.; Escibano, L.; Orfao, A.; Urdiales, J. L. (-)-Epigallocatechin-3-gallate interferes with mast cell adhesiveness, migration and its potential to recruit monocytes. *Cell. Mol. Life Sci.* **2007**, *64*, 2690–2701.
- (7) Melgarejo, E.; Medina, M. A.; Sánchez-Jiménez, F.; Urdiales, J. L. Epigallocatechin gallate reduces human monocyte mobility and adhesion in vitro. *Br. J. Pharmacol.* **2009**, *158*, 1705–1712.
- (8) Swiercz, R.; Skrzypczak-Jankun, E.; Merrell, M. M.; Selman, S. H.; Jankun, J. Angiostatic activity of synthetic inhibitors of urokinase type plasminogen activator. *Oncol. Rep.* **1999**, *6*, 523–526.
- (9) Bachrach, U.; Wang, Y. C. Cancer therapy and prevention by green tea: role of ornithine decarboxylase. *Amino Acids* **2002**, *22*, 1–13.
- (10) Tosetti, F.; Ferrari, N.; De Flora, S.; Albini, A. Angioprevention: angiogenesis is a common and key target for cancer chemopreventive agents. *FASEB J.* **2002**, *16*, 2–14.
- (11) Ho, Y. C.; Yang, S. F.; Peng, C. Y.; Chou, M. Y.; Chang, Y. C. Epigallocatechin-3-gallate inhibits the invasion of human oral cancer cells and decreases the productions of matrix metalloproteinases and urokinase-plasminogen activator. *J. Oral Pathol. Med.* **2007**, *36*, 588–593.
- (12) Albrecht, D. S.; Clubbs, E. A.; Ferruzzi, M.; Bomser, J. A. Epigallocatechin-3-gallate (EGCG) inhibits PC-3 prostate cancer cell proliferation via MEK-independent ERK1/2 activation. *Chem. Biol. Interact.* **2008**, *171*, 89–95.
- (13) Rodríguez-Caso, C.; Rodríguez-Agudo, D.; Sánchez-Jiménez, F.; Medina, M. A. Green tea epigallocatechin-3-gallate is an inhibitor of mammalian histidine decarboxylase. *Cell. Mol. Life Sci.* **2003**, *60*, 1760–1763.
- (14) Bertoldi, M.; Gonsalvi, M.; Voltattorni, C. B. Green tea polyphenols: novel irreversible inhibitors of dopa decarboxylase. *Biochem. Biophys. Res. Commun.* **2001**, *284*, 90–93.
- (15) Moya-García, A. A.; Medina, M. A.; Sánchez-Jiménez, F. Mammalian histidine decarboxylase: from structure to function. *Bioessays* **2005**, *27*, 57–63.
- (16) Moya-García, A. A.; Ruiz-Pernía, J.; Martí, S.; Sánchez-Jiménez, F.; Tuñón, I. Analysis of the decarboxylation step in mammalian histidine decarboxylase. A computational study. *J. Biol. Chem.* **2008**, *283*, 12393–12401.
- (17) Pino-Angeles, A.; Morreale, A.; Negri, A.; Sánchez-Jiménez, F.; Moya-García, A. A. Substrate uptake and protein stability relationship in mammalian histidine decarboxylase. *Proteins* **2010**, *78*, 154–161.
- (18) Hayashi, H.; Mizuguchi, H.; Kagamiyama, H. Rat liver aromatic L-amino acid decarboxylase: spectroscopic and kinetic analysis of the coenzyme and reaction intermediates. *Biochemistry* **1993**, *32*, 812–818.
- (19) Olmo, M. T.; Sánchez-Jiménez, F.; Medina, M. A.; Hayashi, H. Spectroscopic analysis of recombinant rat histidine decarboxylase. *J. Biochem.* **2002**, *132*, 433–439.
- (20) Rodríguez-Caso, C.; Rodríguez-Agudo, D.; Moya-García, A. A.; Fajardo, L.; Medina, M. A.; Subramaniam, V.; Sánchez-Jiménez, F. Local changes in the catalytic site of mammalian histidine decarboxylase can affect its global conformation and stability. *Eur. J. Biochem.* **2003**, *270*, 4376–4387.
- (21) Gervasini, G.; Agundez, J. A.; García-Menaya, J.; Martínez, C.; Cordobés, C.; Ayuso, P.; Cornejo, J. A.; Blanca, M.; García-Martín, E. Variability of the L-Histidine decarboxylase gene in allergic rhinitis. *Allergy* **2010**, *65*, 1576–1584.
- (22) Fukui, H. Progress in allergy signal research on mast cells: up-regulation of histamine signal-related gene expression in allergy model rats. *J. Pharmacol. Sci.* **2008**, *106*, 325–331.
- (23) Burkhard, P.; Dominici, P.; Borri-Voltattorni, C.; Jansson, J. N.; Malashkevich, V. N. Structural insight into Parkinson's disease treatment from drug-inhibited DOPA decarboxylase. *Nat. Struct. Biol.* **2001**, *8*, 963–967.
- (24) Liu, C. Q.; Chen, Z.; Liu, F. X.; Hu, D. N.; Luo, J. H. Involvement of brain endogenous histamine in the degeneration of dopaminergic neurons in 6-hydroxydopamine-lesioned rats. *Neuropharmacology* **2007**, *53*, 832–841.
- (25) Ishikawa, S.; Taira, T.; Niki, T.; Takahashi-Niki, K.; Maita, C.; Maita, H.; Ariga, H.; Iguchi-Ariga, S. M. Oxidative status of DJ-1-dependent activation of dopamine synthesis through interaction of tyrosine hydroxylase and 4-dihydroxy-L-phenylalanine (L-DOPA) decarboxylase with DJ-1. *J. Biol. Chem.* **2009**, *284*, 28832–28844.
- (26) Winblad, B.; Hardy, J.; Backman, L.; Nilsson, L. G. Memory function and brain biochemistry in normal aging and in senile dementia. *Ann. N.Y. Acad. Sci.* **1985**, *444*, 255–268.
- (27) Yates, C. M.; Simpson, J.; Gordon, A. 5-Hydroxytryptamine and dopamine in pre-senile and senile Alzheimer-type dementia. *Biochem. Soc. Trans.* **1990**, *18*, 422–423.
- (28) Schneider, C.; Risser, D.; Kirchner, L.; Kitzmuller, E.; Cairns, N.; Prast, H.; Singewald, N.; Lubec, G. Similar deficits of central histaminergic system in patients with Down syndrome and Alzheimer disease. *Neurosci. Lett.* **1997**, *222*, 183–186.
- (29) Goodsell, D. S.; Morris, G. M.; Olson, A. J. Automated docking of flexible ligands: applications of AutoDock. *J. Mol. Recognit.* **1996**, *9*, 1–5.
- (30) Gordon, J. C.; Myers, J. B.; Folta, T.; Shoja, V.; Heath, L. S.; Onufriev, A. H++: a server for estimating pKas and adding missing hydrogens to macromolecules. *Nucleic Acids Res.* **2005**, *33*, W368–W371.
- (31) Vakser, I. A. Protein docking for low-resolution structures. *Protein Eng.* **1995**, *8*, 371–377.
- (32) Case, D. A.; Darden, T. A.; Cheatham, L. T. E.; Simmerling, C. L.; Wang, J.; Duke, R. E.; Luo, R.; Merz, K. M.; Wang, B.; Pearlman, D. A.; Crowley, M.; Brozell, S.; Tsui, V.; Gohlke, H.; Mongan, J.; Hornak, V.; Cui, G.; Beroza, P.; Schafmeister, C.; Caldwell, J. W.; Ross, W. S.; Kollman, P. A. AMBER 9; University of California: San Francisco, 2006.
- (33) Jorgensen, W. L.; Chandrasekhar, J.; Madura, J.; Impey, R. W.; Klein, M. L. Comparison of simple potential functions for simulating liquid water. *J. Chem. Phys.* **1983**, *79*, 926–935.
- (34) Darden, T. A.; York, D. M.; Pedersen, L. G. Particle mesh Ewald: An N·log(N) method for Ewald sums in large systems. *J. Chem. Phys.* **1993**, *98*, 10089–10092.
- (35) Humphrey, W.; Dalke, A.; Schulten, K. VMD: visual molecular dynamics. *J. Mol. Graph.* **1996**, *14* (33–8), 27–28.
- (36) Gil-Redondo, R.; Estrada, J.; Morreale, A.; Herranz, F.; Sancho, J.; Ortiz, A. R. VSDMIP: virtual screening data management on an integrated platform. *J. Comput.-Aided Mol. Des.* **2009**, *23*, 171–184.
- (37) Moya-García, A. A.; Pino-Ángeles, A.; Gil-Redondo, R.; Morreale, A.; Sánchez-Jiménez, F. Structural features of mammalian histidine decarboxylase reveal the basis for specific inhibition. *Br. J. Pharmacol.* **2009**, *157*, 4–13.
- (38) Medina, M. A.; Urdiales, J. L.; Rodríguez-Caso, C.; Ramírez, F. J.; Sánchez-Jiménez, F. Biogenic amines and polyamines: similar biochemistry for different physiological missions and biomedical applications. *Crit. Rev. Biochem. Mol. Biol.* **2003**, *38*, 23–59.
- (39) Graff, L.; Frungieri, M.; Zanner, R.; Pohlinger, A.; Prinz, C.; Gratzl, M. Expression of histidine decarboxylase and synthesis of histamine by human small cell lung carcinoma. *Am. J. Pathol.* **2002**, *160*, 1561–1565.
- (40) Tanimoto, A.; Matsuki, Y.; Tomita, T.; Sasaguri, T.; Shimajiri, S.; Sasaguri, Y. Histidine decarboxylase expression in pancreatic endocrine cells and related tumors. *Pathol. Int.* **2004**, *54*, 408–412.
- (41) Masliah, E.; Rockenstein, E.; Veinbergs, I.; Mallory, M.; Hashimoto, M.; Takeda, A.; Sagara, Y.; Sisk, A.; Mucke, L. Dopaminergic loss and inclusion body formation in alpha-synuclein mice: implications for neurodegenerative disorders. *Science* **2000**, *287*, 1265–1269.

(42) Carr, G. V.; Lucki, I. The role of serotonin receptor subtypes in treating depression: a review of animal studies. *Psychopharmacology (Berlin)* **2011**, *213*, 265–287.

(43) Leonard, B. E. Serotonin receptors and their function in sleep, anxiety disorders and depression. *Psychother. Psychosom.* **1996**, *65*, 66–75.

(44) Monti, J. M.; Jantos, H. The roles of dopamine and serotonin, and of their receptors, in regulating sleep and waking. *Prog. Brain. Res.* **2008**, *172*, 625–646.

(45) Homberg, J. R.; Contet, C. Deciphering the interaction of the corticotropin-releasing factor and serotonin brain systems in anxiety-related disorders. *J. Neurosci.* **2009**, *29*, 13743–13745.

(46) Bertoldi, M.; Dominici, P.; Moore, P. S.; Maras, B.; Voltattorni, C. B. Reaction of dopa decarboxylase with alpha-methyldopa leads to an oxidative deamination producing 3,4-dihydroxyphenylacetone, an active site directed affinity label. *Biochemistry* **1998**, *37*, 6552–6561.

(47) Fleming, J. V.; Sánchez-Jiménez, F.; Moya-García, A. A.; Langlois, M. R.; Wang, T. C. Mapping of catalytically important residues in the rat L-histidine decarboxylase enzyme using bioinformatic and site-directed mutagenesis approaches. *Biochem. J.* **2004**, *379*, 253–261.